



Article

Mechanical Behavior of Hydroxyapatite-Chitosan Composite: Effect of Processing Parameters

Hamid Ait Said ¹, Hassan Noukrati ^{1,2}, Hicham Ben Youcef ³, Ayoub Bayoussef ^{4,5}, Hassane Oudadesse ⁶ and Allal Barroug ^{1,2,*}

¹ Faculty of Sciences Semlalia, Cadi Ayyad University, 40000 Marrakech, Morocco; aitsaidhamid91@gmail.com (H.A.S.); hassannoukrati@gmail.com (H.N.)

² Centre of Biological and Medical Sciences, Mohammed VI Polytechnic University, CIAM, 43150 Benguerir, Morocco

³ HTMR-Lab, Mohammed VI Polytechnic University, 43150 Benguerir, Morocco; hicham.benyoucef@um6p.ma

⁴ Faculty of Sciences and Technologies, Cadi Ayyad University, 40000 Marrakech, Morocco; a.bayoussef@uhp.ac.ma

⁵ Faculty of Sciences and Technology, Hassan First University of Settat, S3M, 26000 Settat, Morocco

⁶ Campus de Beaulieu, University of Rennes 1, CNRS, ISCR-UMR 6226, F-35000 Rennes, France; hassane.oudadesse@univ-rennes1.fr

* Correspondence: a.barroug@uca.ma; Tel.: +21-262-085-538

Abstract: Three-dimensional hydroxyapatite-chitosan (HA-CS) composites were formulated via solid-liquid technic and freeze-drying. The prepared composites had an apatitic nature, which was demonstrated by X-ray diffraction and Infrared spectroscopy analyses. The impact of the solid/liquid (S/L) ratio and the content and the molecular weight of the polymer on the composite mechanical strength was investigated. An increase in the S/L ratio from 0.5 to 1 resulted in an increase in the compressive strength for HA-CSL (CS low molecular weight: CSL) from 0.08 ± 0.02 to 1.95 ± 0.39 MPa and from 0.3 ± 0.06 to 2.40 ± 0.51 MPa for the HA-CSM (CS medium molecular weight: CSM). Moreover, the increase in the amount (1 to 5 wt%) and the molecular weight of the polymer increased the mechanical strength of the composite. The highest compressive strength value (up to 2.40 ± 0.51 MPa) was obtained for HA-CSM (5 wt% of CS) formulated at an S/L of 1. The dissolution tests of the HA-CS composites confirmed their cohesion and mechanical stability in an aqueous solution. Both polymer and apatite are assumed to work together, giving the synergism needed to make effective cylindrical composites, and could serve as a promising candidate for bone repair in the orthopedic field.

Keywords: chitosan; hydroxyapatite; mechanical strength; composite; bone repair



Citation: Said, H.A.; Noukrati, H.; Ben Youcef, H.; Bayoussef, A.; Oudadesse, H.; Barroug, A. Mechanical Behavior of Hydroxyapatite-Chitosan Composite: Effect of Processing Parameters. *Minerals* **2021**, *11*, 213. <https://doi.org/10.3390/min11020213>

Academic Editor: João Castro-Gomes
Received: 12 December 2020
Accepted: 25 January 2021
Published: 19 February 2021

Publisher's Note: MDPI stays neutral with regard to jurisdictional claims in published maps and institutional affiliations.



Copyright: © 2021 by the authors. Licensee MDPI, Basel, Switzerland. This article is an open access article distributed under the terms and conditions of the Creative Commons Attribution (CC BY) license (<https://creativecommons.org/licenses/by/4.0/>).

1. Introduction

Bone fracture is one of the most common body injuries and is accompanied by social productivity loss, individual disability, and expensive treatment costing billions of dollars per year [1]. The treatment of load-bearing bone defects remains an important barrier for bone engineering. Therefore, the need for biomaterials that can be used in bone repair or as substitutes is apparent. These substances have some important requirements, in terms of biological and physicochemical properties, in order to be successfully used in such situations.

In the orthopedic field, mechanical strength is one of the most crucial characteristics of biomaterials. Thus, these materials must be able to withstand mechanical forces while being continually in contact with bone tissues and fluids. Since these biomaterials are designed to be used as bone implants, it is worth bearing in mind as reference values that the resistance to compression varies from about 90 to 209 MPa and from 1.5 to 45 MPa for human cortical bone and cancellous bone, respectively [2]. Calcium phosphate (CaP) is one of the most common classes of biomaterials investigated for orthopedic applications [3].

This is due to its unique properties, such as biocompatibility, bioactivity, osteoconductivity, and chemical composition, which are comparable with those of bone tissue. Among various forms of CaP materials, particular focus has been given to hydroxyapatite (HA, $\text{Ca}_{10}(\text{PO}_4)_6(\text{OH})_2$), the mineral prototype of calcified tissue, due to its good chemical stability and biological responses in physiological environments. Despite the excellent properties of this apatite, the major drawback is its low mechanical performance, particularly in a porous form [4]. Therefore, this characteristic has typically restrained its applicability to non-load-bearing sites.

Novel strategies such as combinations with polymeric phases to create composite materials and the development of fabrication methods have allowed the partial overcoming of these limitations [2]. Chitosan is one of the most used natural polymers in biomedical applications, particularly in tissue-engineering biomaterials, due to its intrinsic biological properties, such as bioactivity, biocompatibility, low toxicity, and biodegradability [5]. The addition of this biopolymer to CaP apatite formulations is a very powerful approach to better suit the mechanical and physiological demands of the host tissue. Many studies report the impact of CS on the mechanical properties of CaP materials. Compressive strength is the property that is most used to characterize the mechanical behavior of these biomaterials. Techniques such as chemical reaction, lyophilization, coating, and physical mixing are used to fabricate CaP-CS composite biomaterials [6,7]. Although good results were obtained in terms of biological and physicochemical characteristics as well as drug delivery ability, several drawbacks still exist, including the use of large amounts of acidic solutions and cross-linking agents, which could lead to the inflammation of the surrounding tissues [8]. Moreover, higher polymer contents (up to 95 wt%) are usually used to obtain the desired mechanical strength, which makes the treatment more expensive and probably induces toxicity to the human bone tissue [9]. One important aspect worth considering and not explicitly addressed in many of the previous works is the specific role of parameters such as polymer molecular weight and liquid-to-solid ratio in the mechanical strength of CaP-polymer composites, especially hydroxyapatite-chitosan. It is, therefore, crucial to emphasize the need for a thorough investigation of the effect of manufacturing conditions on the mechanical strength and structural features of such composites in order to control and achieve sound knowledge of their mechanical properties.

The present work focuses on the study of the mechanical performance of hydroxyapatite-chitosan (HA-CS) composite material. Thus, the impacts of the fabrication conditions, such as the content and molecular weight of the polymer and liquid/solid (L/S) ratio, are considered and investigated to determine the optimal formulations.

2. Materials and Methods

2.1. Materials

Diammonium hydrogen phosphate ($(\text{NH}_4)_2\text{HPO}_4$, $\geq 99.0\%$) and calcium nitrate tetrahydrate ($\text{Ca}(\text{NO}_3)_2 \cdot 4\text{H}_2\text{O}$, $\geq 99.0\%$) of analytical grade were used as chemical precursors of phosphorus and calcium, respectively. Chitosan (CS) polymer of low (CSL) and medium (CSM) molecular weight (degree of deacetylation higher than 75%) and other products such as acetic acid (CH_3COOH , $\geq 99.7\%$) and ammonium hydroxide (NH_4OH , 25%) were of analytical grade. All the products were obtained from Sigma-Aldrich and used without any further purification. Deionized water was used for preparing all the reactive solutions.

2.2. Hydroxyapatite Synthesis

Hydroxyapatite (HA) solid powder was prepared by co-precipitation between $\text{Ca}(\text{NO}_3)_2 \cdot 4\text{H}_2\text{O}$ and $(\text{NH}_4)_2\text{HPO}_4$ precursors [10]. An aqueous solution of $(\text{NH}_4)_2\text{HPO}_4$ (0.54 mol) was added dropwise to the $\text{Ca}(\text{NO}_3)_2 \cdot 4\text{H}_2\text{O}$ (0.90 mol) aqueous solution containing an excess of ammonium hydroxide (NH_4OH). The system was maintained under constant agitation at around 90 °C. The pH of the medium was about 10. The resulting product was filtered and then dried through lyophilization. Powder with a granulometry of

$\leq 100 \mu\text{m}$ was subsequently used for the formulation of the hydroxyapatite-chitosan (HA-CS) composites.

2.3. Preparation of Hydroxyapatite-Chitosan Composite

The hydroxyapatite-chitosan (HA-CS) composites were formulated by thoroughly mixing the HA precipitated powder with the CS gel solution at a solid to liquid (S/L) ratio of 1. Chitosan solutions (1, 2.5, 5 wt%) were obtained by dissolving an appropriate amount of the chitosan powder in acetic acid solution (2 wt%). The homogenized pastes were sunk in cylindrical molds (8 mm D \times 16 mm H). The samples were frozen and then freeze-dried. In this study, CS with a low and medium molecular weight was used for preparing the specimens; the formulated composites were designated HA-CSL and HA-CSM, respectively. Composites prepared with different CS contents ($x = 1, 2.5, 5 \text{ wt}\%$) were named HA-CSL _{$x\%$} and HA-CSM _{$x\%$} . The effect of the liquid content on the mechanical strength of the composites HA-CSL_{5%} and HA-CSM_{5%} was assessed by varying the value of the S/L ratio (0.5, 0.7, 1).

It is noteworthy that the preparation of cylindrical blocks based only on HA using this technique does not lead to usable samples.

2.4. Physicochemical Characterization

The prepared composite was characterized by X-ray diffraction (XRD) using a X'pert³ Powder Smart Lab diffractometer (Malvern Panalytical, Malvern, UK) with Cu K α radiation ($\lambda = 1.540593 \text{ \AA}$). Data were collected in the 2θ range of 20 up to 70° (2°/min). A Fourier transform infrared (FTIR) analysis was conducted using a Nicolet 5700 spectrometer (ThermoElectron, Waltham, MA, USA) in the range of 400 to 4000 cm^{-1} at a resolution of 4 cm^{-1} . A small amount of the sample powder (1 wt%) was mixed with KBr powder and then palletized onto pallets for analysis.

The microstructure of the specimens was evaluated via scanning electron microscopy (SEM) on a TESCAN VEGA3 microscope (TESCAN, Brno, Czech Republic) and the porosimetry on a Poresizer Micromeritics (Pore Sizer 9310, Micromeritics, Norcross, GA, USA).

2.5. Mechanical Properties

Compressive strength measurements were performed on the formulated cylindrical composites (8 mm D \times 16 mm H) at a crosshead speed of 1 $\text{mm}\cdot\text{min}^{-1}$ using a Universal Testing Machine (Instron 3369, Instron, Norwood, Norfolk, Canton, MA, USA). The compressive strength of the HA-CS (5 wt% of CS) formulations was also measured, in the same conditions, after immersion in KCl (1 mM) aqueous solution. After a predetermined period of time (1 and 7 days), the specimens were removed from the medium and freeze-dried overnight to test the mechanical strength. For each composition, at least three samples were tested.

3. Results and Discussion

Figure 1 shows the diffractograms of HA-CSM composites containing different CSM amounts (2.5 and 5 wt%) compared to HA and CSM. The diffractogram of HA exhibits relatively sharp and defined peaks, characteristic of a relatively well-crystallized specimen; the diffraction peaks can be indexed as apatite phase [11], which matched well with that of pure hydroxyapatite (JCPDS file data, No. 09-432). However, the CSM sample shows only one halo from about 18 to 23°, suggesting the amorphous character of the biopolymer. The XRD patterns of the examined HA-CSM (2.5 and 5 wt% of CSM) show similar patterns, with the presence of the major peaks of the parent material. The major peaks were distinct and fairly sharp, suggesting that the samples were relatively crystalline. The peaks of the CSM polymer are not detected in the HA-CSM diffractograms; this could be attributed to the small amount of polymer introduced in the matrix. It is noted that there was no marked difference with the XRD patterns of the composite containing low molecular weight

chitosan (data not shown), indicating that the polymer molecular weight does not affect the composite structure.

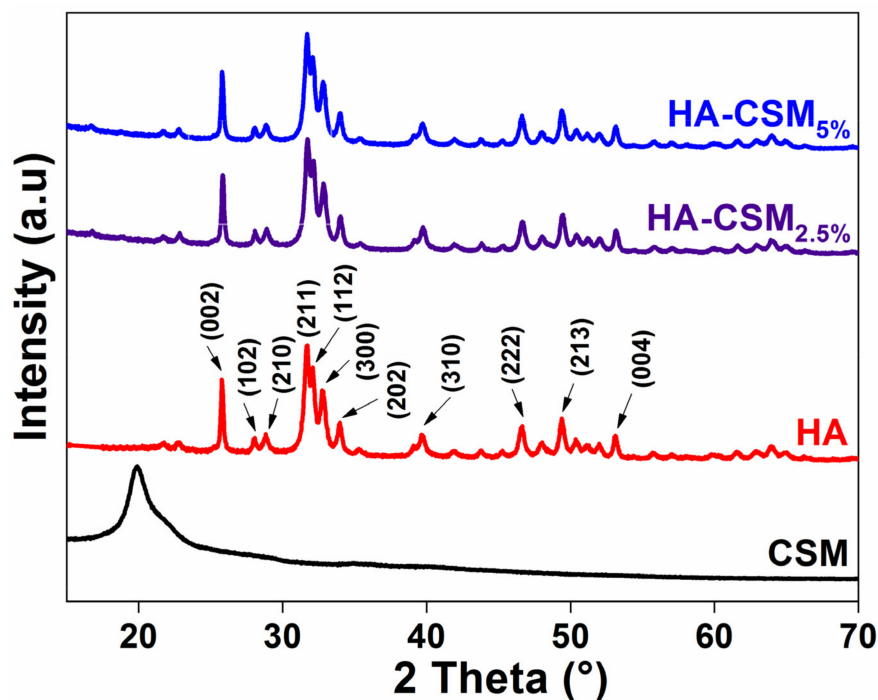


Figure 1. XRD patterns of chitosan (CSM), hydroxyapatite (HA), and hydroxyapatite-chitosan composites (HA-CSM).

The crystallinity degree of the HA-CSM_{2.5%} and HA-CSM_{5%} composites and the HA apatite was determined using the formula:

$$\beta_{002} \times \sqrt[3]{X_C} = K_A, \quad (1)$$

where β_{002} (°) and X_C are the width peak at the half intensity of (002) reflection and crystallinity degree, the constant K_A is set at 0.24 [12]. The addition of the CS polymer in the composite matrix has a slight effect on the composite crystallinity. Thus, the highest value of the crystallinity index is observed for the HA (0.60), whereas this parameter was about 0.58 and 0.55 for the HA-CSM_{2.5%} and HA-CSM_{5%} composites, respectively. This diminution in the composite crystallinity can be explained by the increase in the organic phase content known for its low crystallinity.

The average crystallite size was estimated according to the Scherer equation:

$$L = \frac{K\lambda}{\beta_{002}\cos\theta} \quad (2)$$

where L is the average crystallite size, K is a constant determined by the crystallite shape equal to unity, and λ is the wavelength of X-ray radiation (Cu $K\alpha$ radiation ($\lambda = 1.540593 \text{ \AA}$)). β_{002} (rad) is the full-width peak at the half intensity of (002) reflection. The crystallite size of all the examined composites varies between 28.6 and 29.5 nm, confirming the nanostructure of the composites. The average crystallite sizes were in the order of HA (29.5 nm) > HA-CSM_{2.5%} (29.4 nm) > HA-CSM_{5%} (28.6 nm), suggesting that the addition of the polymer led to a slight decrease in the crystallite size.

The FTIR spectra of the prepared composites HA-CSM (2.5 and 5 wt%) as compared to the reference materials are illustrated in Figure 2. The HA spectrum showed bands characteristic of the phosphocalcic apatite. The PO_4^{3-} vibration modes were observed at around 603–571 cm^{-1} (ν_4), 962 cm^{-1} (ν_1), and 1041–1107 cm^{-1} (ν_3). OH vibrations

with a weak intensity were observed at 633 cm^{-1} and 3579 cm^{-1} [13]. The vibration bands noticed at 3300 cm^{-1} and 1640 cm^{-1} were related to water molecules. The band with a low intensity at 875 cm^{-1} might be attributed to HPO_4^{2-} species, suggesting the non-stoichiometric character of the HA specimen [10]. A comparison between the HA apatite and HA-CS composite spectra confirmed the successful combination of the HA apatite and the polymeric phase. In addition to the HA bands, the HA-CS spectrum indicated the presence of new bands assigned to the CS polymeric phase. Thus, the band attributed to the N-H primary amino group of the polymer was observed at 1572 cm^{-1} . A C-H band related to the CS backbone was observed at 1425 cm^{-1} . Moreover, the band appearing at 1626 cm^{-1} was attributed to the C-O vibration [14].

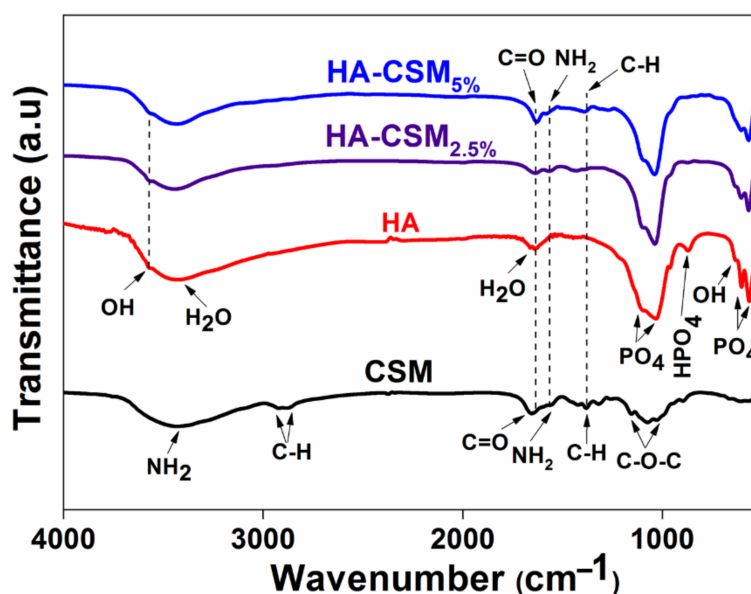


Figure 2. FTIR spectra of chitosan (CSM), hydroxyapatite (HA), and hydroxyapatite-chitosan composites (HA-CSM).

SEM micrographs of the HA-CSM_{5%} composite (Figure 3) revealed a porous structure. The cluster of the apatite layer covered the polymer fibers fully, indicating a good component integration. Moreover, the surface of the HA-CSM composite appeared rough, and few polymer binders with a fibrous-shaped structure are visible. Such morphology could be due to the existence of strong chemical interaction between the CS gel and the HA apatite and to the ability of the polymer to bind the solid particles.

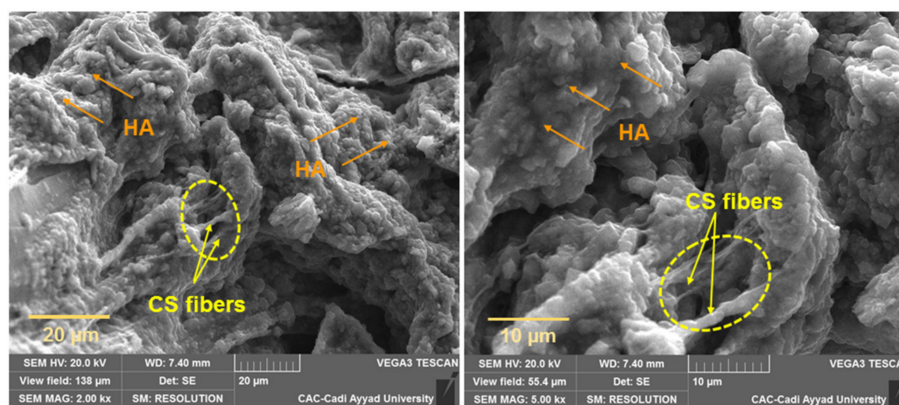


Figure 3. SEM images of the HA-CSM_{5%} composite (5 wt% of CSM) formulated at S/L of 1.

The porosity analysis conducted for the HA-CSM block composites demonstrated that the total pore volume of the formulated composites was affected by the CS addition and the S/L ratio variation. For a S/L ratio of 1, an increase in the polymer content from 1 to 5 wt% led to a decrease in the total pore volume of the composite matrix from 592 to 479 mm³/g, suggesting that the pores are congested by the biopolymer. The change in the solid to the liquid ratio from 0.5 up to 1 reduced the pore volume of the composites from 723 to 479 mm³/g. The use of a large amount of the liquid phase (lower value of S/L) may cause a high dispersion of the solid particles, and this results in a porous structure of the composite when they are freeze-dried.

The mechanical behavior of the formulated HA-CS composites was determined by measuring their compressive strength under various formulation conditions (S/L, content, and molecular weight of the polymer). The evolution of the HA-CS (5 wt% of CS) composite compressive strength as a function of the S/L ratio and the polymer molecular weight is given in Figure 4. The results revealed that the compressive strength of the HA-CSL_{5%} composite increased from 0.08 ± 0.02 to 1.95 ± 0.39 MPa as the S/L ratio rose from 0.5 to 1. The compressive strength noticed for the composite HA-CSM_{5%} takes a low value (0.30 ± 0.06 MPa) when the S/L ratio is 0.5, whereas this mechanical parameter increases abruptly to 2.40 ± 0.51 MPa when the S/L ratio changes to 1. This could be argued considering the decrease in the porosity of the composite matrix when increasing the S/L ratio. As the liquid content is high (S/L of 0.5), the cohesion within the components might be destroyed, resulting in a poor mechanical strength. It is generally established that a high S/L value leads to a low porosity and high mechanical strength, while a low S/L has an opposite effect [15,16]. For instance, the compressive strength of the CaP bone cement is pronouncedly increased from 21.0 ± 2.5 to 48.0 ± 2.3 MPa as the liquid to solid ratio (L/S) decreased from 0.6 to 0.3.

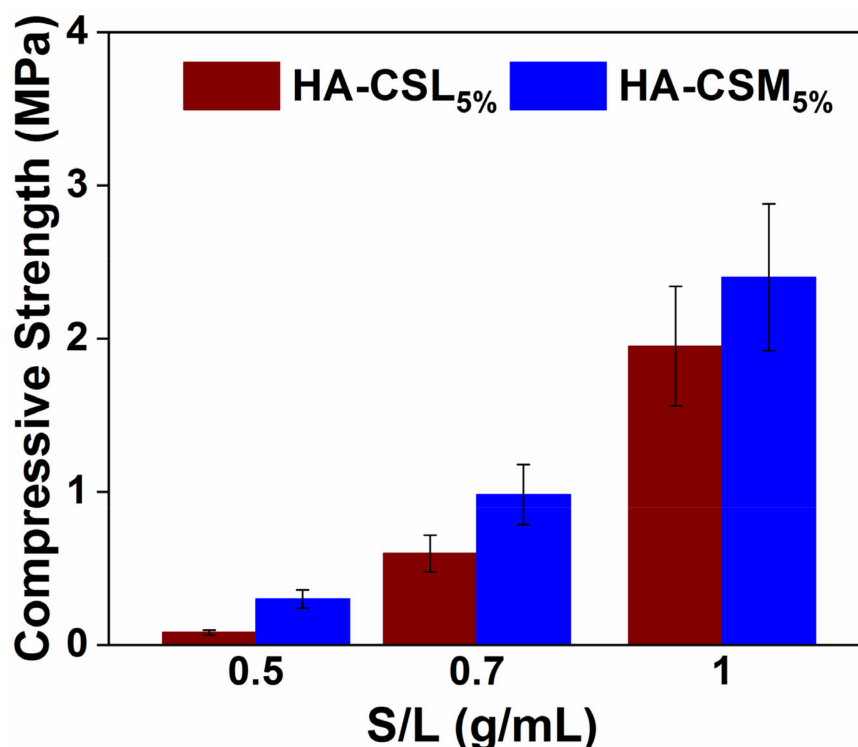


Figure 4. Effect of the solid to liquid (S/L) ratio (0.5, 0.7, and 1) and polymer molecular weight on the compressive strength of the HA-CSL_{5%} and HA-CSM_{5%} (5 wt% of CS) composites.

The compressive strength of the HA-CSM and HA-CSL composites was slightly affected by the polymer molecular weight (Figure 4). This property improves when the CS molecular weight increases, no matter what the S/L ratio (0.5, 0.7, or 1). For a

S/L ratio of 0.5, the compressive strength of the HA-CSM_{5%} composite (0.3 ± 0.06 MPa) was approximately four times higher than that of HA-CSL_{5%} (0.08 ± 0.016 MPa). A similar trend was observed when the L/S ratio was set at 0.7 or 1. The composite HA-CSM_{5%} formulated at an S/L of 1 displays the highest compressive strength value of 2.40 ± 0.48 MPa, somewhat greater than that of HA-CSL_{5%} (1.95 ± 0.39 MPa). These results could be understood in terms of the length of the polymer chains and their role in binding the apatite particles. The slightly higher compressive strength of the HA-CSM composite compared to HA-CSL might be attributed to the longer polymeric chains and more functional groups, which served as specific sites for chemical interaction with the inorganic particles.

It is worth to note that at a ratio of S/L higher than 1, the composite pastes were unobtainable because the manufacturing process was difficult as a result of the paste being too dry during mixing. Unfortunately, increasing the S/L ratio to a value higher than 1 is not a good strategy to enhance the compressive strength of the examined composite.

The effect of the content and molecular weight of the polymer on the composite compressive strength was examined for a S/L ratio of 1. The latter was selected for better cylindrical composite cohesiveness and mechanical strength. The value of the compressive strength improves with the increase in the CS amount, and this effect is graphically illustrated in Figure 5. For example, the compressive strength of the HA-CSM composite rose from 0.51 ± 0.10 to 2.40 ± 0.48 MPa as the CSM content increased from 1 to 5 wt%. This variation was mainly due to the diminution in the total pore volume (from 592 to 479 cm³/g) as the CSM content increased (from 1 to 5 wt%). A similar tendency occurred for the composites formulated with a low molecular weight. The strengthening of the composite structure could be due to the high Ca-binding ability of the polymer, which could tightly bind the HA particles together with polymeric chains, and the results indicate the good cohesion and strength of the composite.

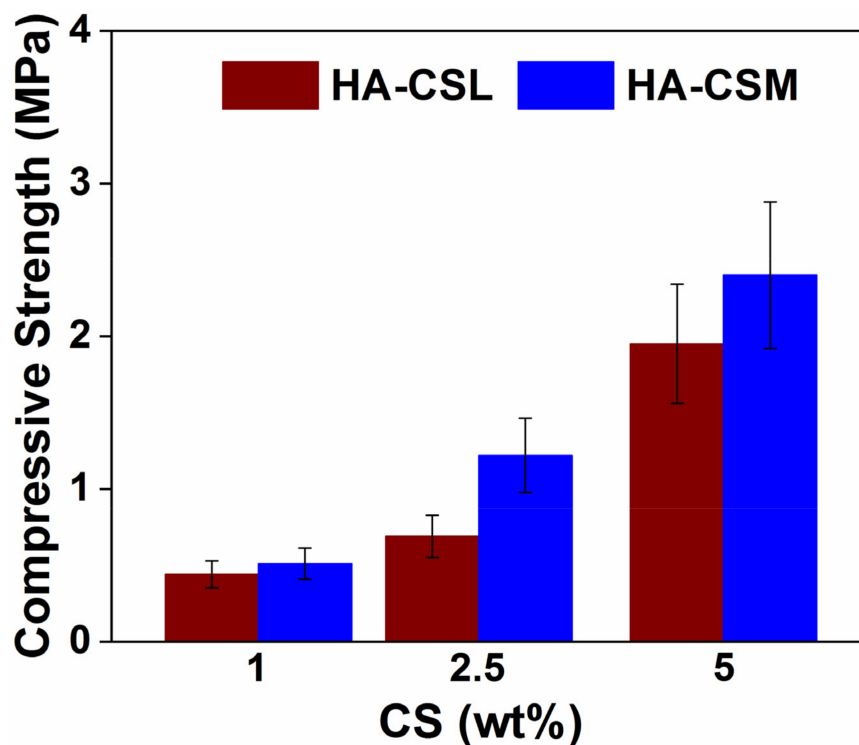


Figure 5. Influence of the polymer content (1, 2.5, and 5 wt%) and the molecular weight on the compressive strength of the HA-CS composites formulated at a S/L value of 1.

Moreover, the results indicated that an increase in the CS molecular weight from low to medium value provokes an improvement in the composite compressive strength, whatever the percentage of the polymer (1, 2.5, or 5 wt%) in the composite.

It is noteworthy that the HA-CSM_{5%} specimen formulated with the medium polymer molecular weight and the highest S/L ratio (S/L ~1) exhibited the highest compressive strength value of about 2.40 ± 0.48 MPa as compared with the other formulations.

To evaluate the cohesiveness of the formulated cylindrical composites (HA-CSL_{5%} and HA-CSM_{5%}), the compressive strength was measured after immersion in a KCl (1 mM) aqueous solution as a simple and stable medium. The polymer content of 5 wt% and S/L ratio of 1 were selected in this study to maintain the mechanical strength as high as possible. The results reported in Figure 6 indicate that no significant difference was found in the compressive strength at different periods of time. The mean values of the compressive strength were, respectively, about 2.40 ± 0.34 MPa and 1.94 ± 0.27 MPa for HA-CSM_{5%} and HA-CSL_{5%}, confirming the ability of the cylindrical composites to keep their geometrical integrity after immersion in the aqueous solution. This might also be the result of the strong chemical interaction between the inorganic and organic phases within the matrix of the composites. It should be noted that the cohesion property of the formulated cylindrical composites is one of the important parameters that needs to be considered for clinical applications. A poor cohesion of the CaP paste may lead to a negative in vivo response and inflammatory reactions due to the elution of microparticles from the material [17].

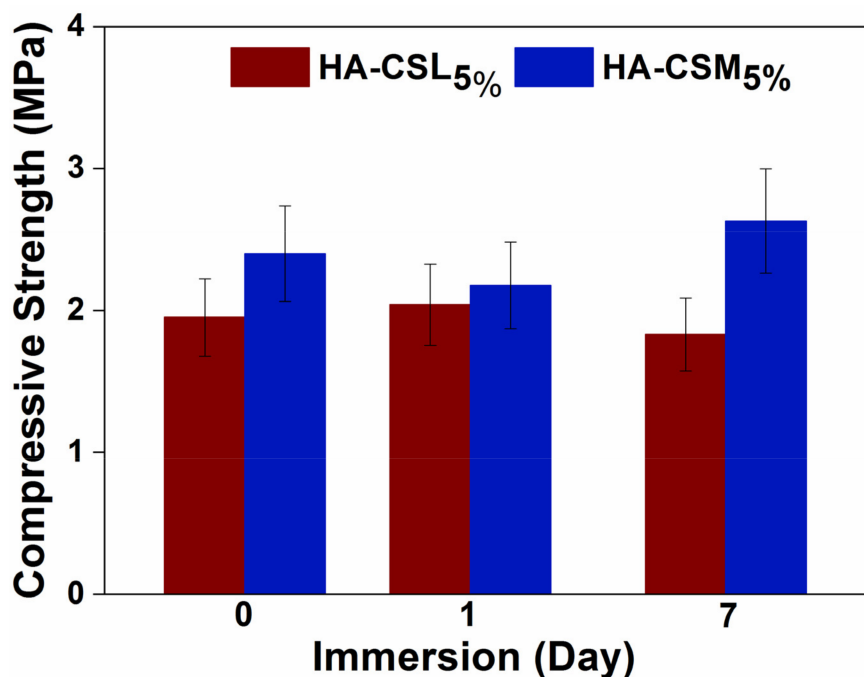


Figure 6. Compressive strength of the HA-CSL_{5%} and HA-CSM_{5%} composites after immersion in KCl (1 mM) aqueous solution.

From the overall results obtained, it is clear that the combination of CS polysaccharide with HA is an appealing strategy to improve the mechanical strength of the apatite matrix. Both the polymer and HA apatite phases are assumed to work together, giving a synergism needed to make effective HA-CS cylindrical composites with sufficient and stable compressive strength. Moreover, the variation in various formulation conditions (content and molecular weight of the CS and solid-to-liquid ratio) plays a crucial role in controlling the compressive strength of the composite. The obtained compressive strength values are comparable to those reported for cancellous bone (1.5–45 MPa) [2]. Hence, the formulated composites could be promising biomaterials for biomedical applications in bone defect repair.

4. Conclusions

A three-dimensional hydroxyapatite-chitosan (HA-CS) composite was prepared by a solid-liquid mixing method combined with lyophilization. The effect of different formulation conditions, including the content and molecular weight of the polymer as well as the solid to the liquid ratio, on the composite compressive strength was investigated. An increase in the S/L ratio provoked an improvement in the composite compressive strength of the examined composite. However, an augmentation in the content and molecular weight of the polymer increases the compressive strength of the composite. The HA-CS specimens formulated with the largest polymer content (5 wt%) and the highest S/L ratio (S/L ~1) had the highest compressive strength. The strengthening effect of the polymeric additive could be due to the strong interaction between the inorganic and polymeric phases during the formulation and the reduction in the porosity. The developed composite exhibits qualities that individual apatite does not possess. However, matching the mechanical strength of the bone is not sufficient to make a successful bone implant, as the biological properties (biocompatibility, biodegradability . . .) also have to be considered. Thus, it is vital to conduct profound in vitro and in vivo studies on the devolved composite before any application as a future bone implant.

Author Contributions: Conceptualization, H.N. and H.A.S.; Methodology, H.A.S. and H.N.; Validation, A.B., H.O., H.N., H.B.Y.; Formal analysis, H.A.S. and A.B. (Ayoub Bayoussef); Investigation, H.A.S. and H.N.; Supervision, H.B.Y., H.O. and A.B. (Allal Barroug); Writing—original draft, H.A.S. and H.N.; Writing—review & editing, H.N., H.B.Y., H.O. and A.B. (Allal Barroug); Visualization, H.N. and H.A.S.; Supervision, A.B (Allal Barroug), and H.O. All authors have read and agreed to the published version of the manuscript.

Funding: This research received no external funding.

Data Availability Statement: Not applicable.

Acknowledgments: This work was supported by OCP Foundation via the R&D Initiative «Appel à projets autour des phosphates, APPHOS» under the project ID: MAT-BAR-01/2017. The authors would like to thank OCP Foundation, OCP Innovation, UM6P, CNRST, MESRSFC, and Center of Analysis and Characterization (CAC) of UCA (Morocco). The authors are also grateful to R. Hakkou from UCA, for his assistance in conducting the mechanical measurement.

Conflicts of Interest: The authors declare no conflict of interest.

References

1. Ghiasi, M.S.; Chen, J.; Vaziri, A.; Rodriguez, E.K.; Nazarian, A. Bone fracture healing in mechanobiological modeling: A review of principles and methods. *Bone Rep.* **2017**, *6*, 87–100. [[CrossRef](#)] [[PubMed](#)]
2. Ginebra, M.P.; Montufar, E.B. Cements as bone repair materials. In *Bone Repair Biomaterials*; Pawelec, M.K., Planell, A.J., Eds.; Elsevier: Amsterdam, The Netherlands, 2019; pp. 233–271.
3. Dorozhkin, S.V. Multiphasic calcium orthophosphate (CaPO₄) bioceramics and their biomedical applications. *Ceram. Int.* **2016**, *42*, 6529–6554. [[CrossRef](#)]
4. Kwon, S.H.; Jun, Y.K.; Hong, S.H.; Lee, I.S.; Kim, H.E.; Won, Y.Y. Calcium Phosphate Bioceramics with Various Porosities and Dissolution Rates. *J. Am. Ceram. Soc.* **2004**, *85*, 3129–3131. [[CrossRef](#)]
5. Oudadesse, H.; Wers, E.; Bui, X.V.; Roiland, C.; Bureau, B.; Akhiyat, I.; Mostafa, A.; Chaair, H.; Benhayoune, H.; Fauré, J.; et al. Chitosan effects on glass matrices evaluated by biomaterial MAS-NMR and biological investigations. *Korean J. Chem. Eng.* **2013**, *30*, 1775–1783. [[CrossRef](#)]
6. Peniche, C.; Solís, Y.; Davidenko, N.; García, R. Chitosan/hydroxyapatite-based composites. *Biotechnol. Appl.* **2009**, *27*, 202–210.
7. Boudemagh, D.; Venturini, P.; Fleutot, S.; Cleymand, F. Elaboration of hydroxyapatite nanoparticles and chitosan/hydroxyapatite composites: A present status. *Polym. Bull.* **2019**, *76*, 2621–2653. [[CrossRef](#)]
8. Casey, M.L.; Hawley, B.; Edwards, N.; Cox-Ganser, J.M.; Cummings, K.J. Health problems and disinfectant product exposure among staff at a large multispecialty hospital. *Am. J. Infect. Control* **2017**, *45*, 1133–1138. [[CrossRef](#)] [[PubMed](#)]
9. Wiegand, C.; Winter, D.; Hippler, U.C. Molecular-Weight-Dependent Toxic Effects of Chitosans on the Human Keratinocyte Cell Line HaCaT. *Skin Pharmacol. Physiol.* **2010**, *23*, 164–170. [[CrossRef](#)] [[PubMed](#)]
10. Errassifi, F.; Sarda, S.; Barroug, A.; Legrouri, A.; Sfihi, H.; Rey, C. Infrared, Raman and NMR investigations of risedronate adsorption on nanocrystalline apatites. *J. Colloid Interface Sci.* **2014**, *420*, 101–111. [[CrossRef](#)] [[PubMed](#)]

11. Louihi, S.; Noukrati, H.; Tamraoui, Y.; Said, H.A.; Ben Youcef, H.; Manoun, B.; Barroug, A. Adsorption and structural properties of hydroxy- and new lacunar apatites. *J. Mol. Struct.* **2020**, *1202*, 127225. [[CrossRef](#)]
12. Rusu, V.; Ng, C.; Wilke, M.; Tiersch, B.; Fratzl, P.; Peter, M. Size-controlled hydroxyapatite nanoparticles as self-organized organic-inorganic composite materials. *Biomaterials* **2005**, *26*, 5414–5426. [[CrossRef](#)] [[PubMed](#)]
13. Rey, C.; Shimizu, M.; Collins, B.; Glimcher, M.J. Resolution-enhanced fourier transform infrared spectroscopy study of the environment of phosphate ions in the early deposits of a solid phase of calcium-phosphate in bone and enamel, and their evolution with age. I: Investigations in the ν_4 PO₄ domain. *Calcif. Tissue Int.* **1990**, *46*, 384–394. [[CrossRef](#)] [[PubMed](#)]
14. Queiroz, F.M.; Melo, T.R.K.; Sabry, A.D.; Sasaki, L.G.; Rocha, O.A.H. Does the Use of Chitosan Contribute to Oxalate Kidney Stone Formation? *Mar. Drugs* **2014**, *13*, 141–158. [[CrossRef](#)] [[PubMed](#)]
15. Ginebra, M.P.; Canal, C.; Espanol, M.; Pastorino, D.; Montufar, E.B. Calcium phosphate cements as drug delivery materials. *Adv. Drug Deliv. Rev.* **2012**, *64*, 1090–1110. [[CrossRef](#)] [[PubMed](#)]
16. Zhou, Z.; Ye, D.; Liang, W.; Wang, B.; Zhu, Z. Preparation and characterization of a novel injectable strontium-containing calcium phosphate cement with collagen. *Chin. J. Traumatol.* **2015**, *18*, 33–38. [[CrossRef](#)] [[PubMed](#)]
17. Tsai, Y.F.; Wu, C.C.; Fan, F.Y.; Cheng, H.C.; Liaw, Y.C.; Huang, Y.K.; Hsu, L.H.; Yang, K.C. Effects of the addition of vancomycin on the physical and handling properties of calcium sulfate bone cement. *Process Biochem.* **2014**, *49*, 2285–2291. [[CrossRef](#)]